

## **Mechanical properties of pulsed laser deposited nanocrystalline SiC films**

D. Craciun<sup>a</sup>, G. Socol<sup>a</sup>, D.V. Cristea<sup>b</sup>, M. Stoicanescu<sup>b</sup>, N. Olah<sup>c</sup>, K. Balazsi<sup>c</sup>, N. Stefan<sup>a</sup>, E. Lambers<sup>d</sup>, V. Craciun<sup>a,\*</sup>

<sup>a</sup>National Institute for Laser, Plasma, and Radiation Physics, Magurele, Romania

<sup>b</sup>Transilvania University, Brasov,

<sup>c</sup>Romanian Institute for Technical Physics and Materials Science, Budapest, Hungary

<sup>d</sup>Major Analytical Instrumentation Center, University of Florida, Gainesville, FL 32611, USA

### **Abstract**

The mechanical properties of nanocrystalline SiC thin films grown on (100) Si at a substrate temperature of 1000°C under a CH<sub>4</sub> atmosphere using the pulsed laser deposition (PLD) technique were investigated. Nanoindentation results showed that films exhibited hardness values around 36 GPa and Young modulus values around 250 GPa. Scratch tests found that films were adherent to the substrate, with critical load values similar to those recorded for other hard coatings deposited on significantly softer Si substrates. Wear tests performed at a temperature of 900°C showed that films exhibited friction coefficients and wear rates very similar to those measured at room temperature, due to the presence of C–C bonds as evidenced by X-ray photoelectron spectroscopy investigations. These results recommend such coatings for demanding high temperature applications such as nuclear fuel encapsulation.

### **1. Introduction**

Due to its excellent mechanical, optical, thermochemical, electronic and electrical properties SiC has been extensively investigated for potential uses in microelectronics [1,2], hard and protective coatings for tools [3,4], water splitting [5] and bio-applications [6]. More recently, it has been suggested that due to its very low neutron absorption cross section, SiC could be used in the nuclear industry as encapsulating coatings for nuclear fuel in next generation reactors [7,8]. For such applications the deposited SiC films are expected to maintain their properties at temperatures between 500 and 800°C and even higher, up to 1000°C, in the case of an emergency if an accident occurs. The deposition of high quality SiC films to study their properties is a challenging process due to their low sputtering yield, high melting temperature and reactivity with oxygen [1–4]. Progress has been recently made using CVD, ion beam or sputtering techniques [1–8]. By using the Pulsed Laser Deposition (PLD) technique, good quality SiC films that are very useful for properties investigations were also synthesized [9–14]. The use of a high laser fluence, a very low residual vacuum, high purity CH<sub>4</sub> and high repetition rates were necessary to grow the films [15]. Results obtained from simulations of the X-ray reflectivity curves acquired from the PLD grown films showed that they possess a low surface roughness (rms values < 1 nm) and a density around 3.20 g/cm<sup>3</sup>, almost identical to the tabulated value for bulk SiC. Grazing incidence X-ray diffraction studies showed the films were nanocrystalline while X-ray photo-electron

spectroscopy investigations found that films contained in bulk a rather low oxygen concentration, below 2–3 at.%. The results of systematic nanoindentation investigations and wear tests performed at room temperature and 900°C on PLD grown SiC films are presented below.

2. Experimental details

The PLD experimental set up used to deposit films has been described previously [15]. It uses a KrF excimer laser ( $\lambda = 248$  nm, pulse duration  $\tau_p = 25$  ns, 8 J/cm<sup>2</sup> fluence, 40 Hz repetition rate) to ablate SiC polycrystalline targets (Angstrom Sciences) in a stainless steel chamber. The ultimate pressure in the deposition chamber was in the low 10<sup>-6</sup> Pa. Since the properties of the deposited films improved with the increase of the substrate temperature, we restricted our investigations to films deposited using the maximum temperature of 1000°C achievable in our deposition system. Moreover, because the wear testing of such films involved experiments at 900°C, it was not very useful to deposit them at lower temperatures. Series of films were deposited at 1000°C on Si substrates (MEMC Electronic Materials, Inc.) for 27,000 and 14,000 pulses (generic names SiC 17 and SiC 18, respectively) under a high purity of  $2 \times 10^{-5}$  mbar of CH<sub>4</sub>. After deposition, films underwent a 1 h anneal at the deposition temperature and then were slowly cooled at room temperature at a rate of 5°C/min. As mentioned in the Introduction part, the crystalline structure, surface roughness, mass density, elemental composition, and optical properties of these films were previously reported [15]. According to ellipsometry measurements, the thickness of the deposited films were around 1  $\mu$ m and 0.5  $\mu$ m,  $\pm 5\%$  on an area of 2 cm<sup>2</sup> for the SiC 17 and SiC 18 series of samples, respectively. The mechanical properties of the thin films were investigated using a nanoindentation device produced by CSM Instruments (NHT-2) equipped with a Berkovich diamond tip. To minimize substrate contributions, the indentation experiments were performed controlling the depth penetration of the indenter, between 80 and 120 nm and 40 and 150 nm at maximum loads ranging from  $\sim 4$  to  $\sim 7$  mN and  $\sim 1$  to  $\sim 11$  mN for samples SiC 17 and samples SiC 18, respectively. The hardness and reduced modulus were determined following the model of Oliver and Pharr [16]. On each series of samples, a matrix of measurements, with X and Y displacements of 0.05 mm, have been made, with the following protocol: linear loading, loading rate = 100 nm/min, pause during full load 2 s (in order to minimize the creep effect), and unloading rate = 100 nm/min. Considering the thickness variation of PLD grown films only the indentations that were located on the central area of the films were taken into consideration. The load resolution of the apparatus is 40 nN, with a usable indentation load range between 0.1 and 500 mN. The thermal drift, which can influence the measurements with indentation depths lower than 100 nm, is countered with the use of a zirconium reference ring, which is in contact with the sample surface. The reference ring also acts as a local environmental enclosure to passively protect the measurement location from air currents, sound waves and changes in humidity and temperature. Furthermore the environmental temperature and humidity are kept constant during measurement sessions. For comparison purposes, nanoindentation measurements were performed on the silicon substrate, with the following protocol: Berkovich diamond indenter, linear loading, 300 nm penetration depth, loading and unloading rates of 1000 nm/min. The scratch tests were performed on a Micro Scratch Tester (CSM Instruments) using a 100Cr6 steel tipped indenter with a Rockwell geometry (tip radius = 100  $\mu$ m). The load was applied progressively, from 0.03 N to 9 N for samples SiC 17, and from 0.03 to 8 N for samples SiC 18, with a speed of 1 N/min. The length of the tests was set at 3 mm, being confined to the samples' area of relatively uniform thickness. Three tracks were made on each measured sample, with a displacement on the Y axis of 0.2 mm between each track. The critical load values were obtained after optical analysis of the wear tracks, and these are defined as follows: Lc1– the load necessary for the emergence of the first cracks in the film; Lc2– the load corresponding to the first delamination of the film; Lc3– the load responsible for the delamination of more than 50% of the film from the wear track. Mechanical wear tests were

carried out at 25°C and 900°C in air atmosphere using a dry ball-on-disk tribometer from CSM Instruments. The bearing balls were made out of Si<sub>3</sub>N<sub>4</sub> having a diameter of 5 mm. The normal load was set at 1.00 N, the maximum linear speed at 0.05 m/s and the stop condition at 2400 cycles. The chemical composition of the films was investigated by X-ray photoelectron spectroscopy (XPS) on a Physical Electronics PHI 5000 VersaProbe II using monochromatic Al K<sub>α</sub> radiation (1486.6 eV). Sputtering of the surface was done with 2 kV Ar ions while the sample was rotated to ensure a uniform removal rate.

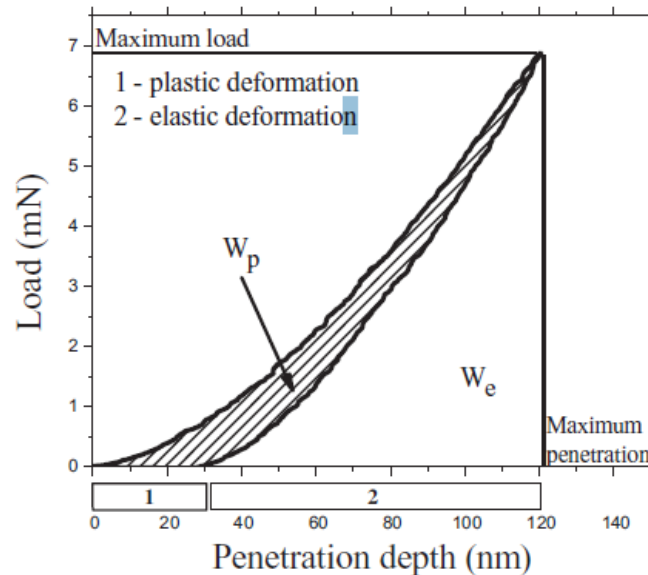


Fig. 1. Loading–unloading curves for a penetration depth of 120 nm recorded for a sample SiC 17.

### 3. Results and discussion

Nanoindentation measurements were performed in multiple locations on several samples, with different penetration depths. The representative results are presented in Table 1. Overall, the results showed that the films were very hard, exhibiting values from ~32 to ~41 GPa for both samples, while the elastic modulus values were around 250–260 GPa, typical values for good quality SiC films [17,18]. However, upon further investigation of the data, several observations can be extracted. Fig. 1 represents a typical loading–unloading curve for a penetration depth of 120 nm recorded for sample SiC 17. From the evolution of the loading–unloading curves, it can be observed that the film exhibited a very small degree of plastic deformation. A similar evolution was noticed for the remaining measurements, regardless of the penetration depth, which leads to the conclusion that the mechanical characteristics are relatively homogeneous throughout the measured thickness of the films. This observation can be supported by a more in-depth analysis of the loading–unloading curves. By analyzing the load–displacement response, one can extract other mechanical metrics apart from the hardness ( $H_{it}$ ), such as the plastic work ratio ( $u_p$ ), defined as:

$$u_p = W_p / W_t \quad (1)$$

where  $W_t$  is the total work of indentation which is separated into an elastic ( $W_e$ ) and a plastic ( $W_p$ ) component (as seen in Fig. 1). These parameters are extracted from the experimentally measured loading–unloading curve. Higher  $u_p$  values denote a material with a higher ability to dissipate energy in plastic deformations. Fig. 2 presents the variation of the plastic work ratio as a function of the penetration depth. One can observe that, for both samples, the plastic work ratio is stabilized in the penetration depth interval 80–120 nm. Following this interval, the

plastic work ratio rises abruptly for the thinner sample up to a value of  $\sim 0.31$ . This phenomenon should be expected, considering that the penetration depth for this particular measurement reaches 30% of the total film thickness (500 nm). The physics and technique of nanoindentation measurements in films thinner than 0.5  $\mu\text{m}$  is still a matter of debate [19,20]. However, considering the plastic work ratio for the silicon substrate (0.50), the fact that the measured hardness for the SiC samples is  $\sim 70\%$  higher than that of the substrate, and the stabilization of the plastic work ratio between the penetration depth 80–120 nm, the reported mechanical values for the SiC films from Table 1 could be taken as an indication of the hardness of these very thin films. One observation that needs to be mentioned is that the variable parameter controlled during the deposition of the samples, the number of the pulses, does not seem to significantly influence either the hardness or the elastic modulus.

**Table 1**

The mechanical characteristics of SiC films obtained by nanoindentation ( $H_{it}$  – indentation hardness;  $E_{it}$  – indentation modulus;  $W_p$  – plastic work;  $W_e$  – elastic work;  $u_p$  – plastic work ratio).

Sample	Penetration depth [nm]	$H_{it}$ [GPa]	$E_{it}$ [GPa]	HV Vickers	$W_p$	$W_e$	$u_p$	H/E	$H^3/E^2$
SiC-17	80	32.6	238	3023	20.60	104.83	0.1965	–	–
	90	34.3	232	3176	27.77	139.01	0.1997	–	–
	120	35.5	239	3290	62.22	325.96	0.1908	–	–
	120	36.2	242	3351	68.62	318.95	0.2151	–	–
	Arithmetic mean value	34.6	237.7	3210	–	–	–	0.14	0.73
	Relative error	$\pm 5.91\%$	$\pm 2.41\%$	$\pm 5.82\%$	–	–	–	–	–
SiC-18	40	32.7	261	3029	1.26	13.23	0.0952	–	–
	80	37.3	259	3456	18.25	119.94	0.1521	–	–
	100	35.6	254	3297	33.52	204.8	0.1636	–	–
	100	35.1	237	3250	30.58	184.05	0.1661	–	–
	150	35.2	285	3258	212.71	697.01	0.3051	–	–
	Arithmetic mean value	35.18	259.2	3258	–	–	–	0.13	0.64
	Relative error	$\pm 7.04\%$	$\pm 9.95\%$	$\pm 7.02\%$	–	–	–	–	–
Si (substrate)	Arithmetic mean value	11.2	130	1042	1034.8	2035.0	0.50	0.08	0.08
	Relative error	$\pm 0.38\%$	$\pm 3.58\%$	$\pm 0.38\%$	$\pm 0.91\%$	$\pm 1.92\%$	$\pm 1\%$	–	–

From the nanoindentation obtained hardness and elastic modulus it is possible to evaluate other important key parameters to analyse the wear behavior of the films. The H/E ratio can provide information about the wear of the films [21], while the  $H^3/E^2$  ratio gives information about the resistance to plastic deformation. Table 1 also contains the values for the H/E and  $H^3/E^2$  ratios for the deposited samples calculated using the average of the measured values. One can notice that, regarding the H/E ratio, the thicker SiC film (sample SiC 17) might behave slightly better during wear tests. In Table 2, the experimentally measured values for the critical loads concerning the adhesion to the substrate, for each track, of each sample, are presented. If we compare the critical load values for each sample, we notice that sample SiC 18, overall, exhibits slightly higher values, therefore a better adhesion to the substrate. Keeping in mind that the main variable while depositing the films on the silicon substrates was the number of pulses, there seems to be a small influence of this parameter on the adhesion to the substrate measurement results. During longer deposition times the entrance window transmittance decreases due to the deposition of a thin film, which in turn decreases the laser fluence incident on the target. Considering the values from Table 2, one could note that the adhesion of the SiC films to the silicon substrate is, in this particular case, lower than that measured for the thinner film. More likely, the explanation regarding the lower adhesion to the substrate stems from the discrepancy of the mechanical characteristics of the Si substrate compared to the ones of the films, a typical case of a very hard film on a soft substrate system. The mechanical characteristics of the substrate are presented in Table 1. This observation is firstly reinforced by the appearance of the scratch tracks. Figs. 3 and 4 represent images captured from the regions where the critical loads concerning the adhesion to the substrate were observed, for sample SiC 17 and sample SiC 18, respectively. According to Ref. [22], the shape (chevrons) and orientation of the cracks (open to the direction of the scratch)

from Figs. 3 and 4 are characteristic to the process called through-thickness cracking. This phenomenon is usually followed by recovery spallation (as is the case for these particular SiC samples), where the coating is delaminated due to the elastic recovery which occurs behind the stylus as it travels over the coated surface. One observation that needs to be mentioned is that, in this particular case, the  $L_{c3}$  critical load is not necessarily related to the definition (the load where more than 50% of the film is delaminated from the substrate), but represents the cohesive failure of the thin film-substrate system, due to crack-ing occurred also in the substrate.

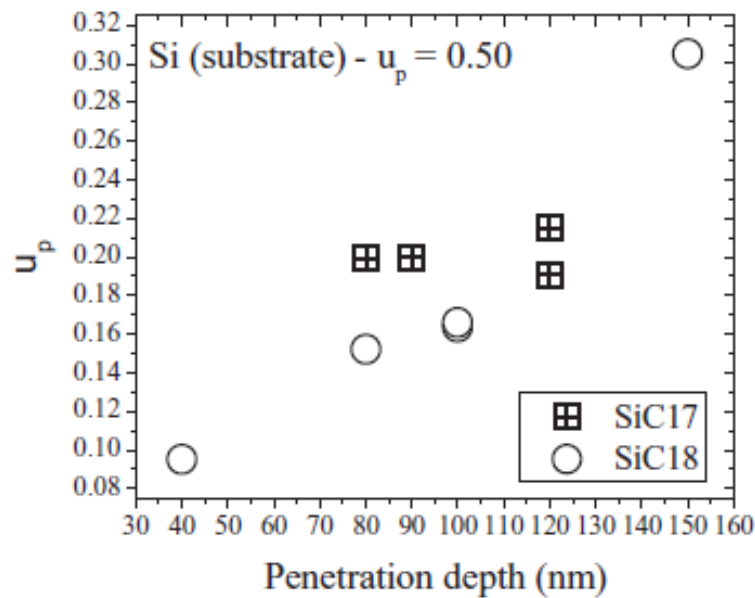


Fig. 2. The variation of the plastic work ratio as a function of the penetration depth.

Consequently, the relatively high measuring error for the  $L_{c3}$  load, in the case of sample Si 17, is not conclusive concerning the adhesion behavior, firstly due to the lack of thin film-substrate system cohesion and also accounting for the fact that past critical load  $L_{c2}$  the film is already considered compromised. Secondly, the observed critical load values were very similar to those measured for other pairs of hard film-soft substrate such as ZrC/Si and ZrN/Si [23,24].

Table 2 The critical load values resulted from the adherence tests on samples SiC 17 and SiC 18.

Sample	Track	$L_{c1}$ [N]	$L_{c2}$ [N]	$L_{c3}$ [N]
SiC_17	1	2.47	3.91	7.61
	2	2.63	4.64	5.43
	3	2.64	3.80	5.11
	Arithmetic mean value	2.58	4.11	6.05
	Relative error	±4.26%	±12.89%	±25.78%
SiC_18	1	3.09	4.23	7.59
	2	2.58	4.32	7.43
	3	2.79	4.07	7.55
	Arithmetic mean value	2.82	4.20	7.52
	Relative error	±8.51%	±3.09%	±1.19%

Examples of the recorded friction coefficients and penetration depths during wear tests recorded for sample SiC 17 at room temperature and 900°C are displayed in Fig. 5. The estimated values of the worn material as well as the wear rate for both samples are displayed in Table 3. The surface behavior of samples during tests is different if different temperatures are used. In the first case (room temperature), the first part of curve shown in Fig. 5, left (1–182 s) was influenced by the inhomogeneity and roughness of the surface, the next part (plateau) being representative of the actual friction coefficient. For the high temperature test, even if the used 900°C temperature was very high, it is obvious that the SiC 17 film was destroyed after a similar length (around 17.30 m, 1.44E03 laps) as in the case of room temperature testing. The thinner SiC 18 sample exhibited a slightly higher worn volume and friction coefficient average values, although the critical loads values were higher. There are two important results from these tests: first, the friction coefficients measured for these nanostructured thin SiC films were in line with other measurements reported in the literature for much thicker SiC films or bulk samples [25–27]. Secondly, there were no major differences between the wear properties measured at room temperature and those measured at 900°C. These results showed that the SiC films could maintain their mechanical properties at very high temperatures, making them attractive for special applications in nuclear reactors.

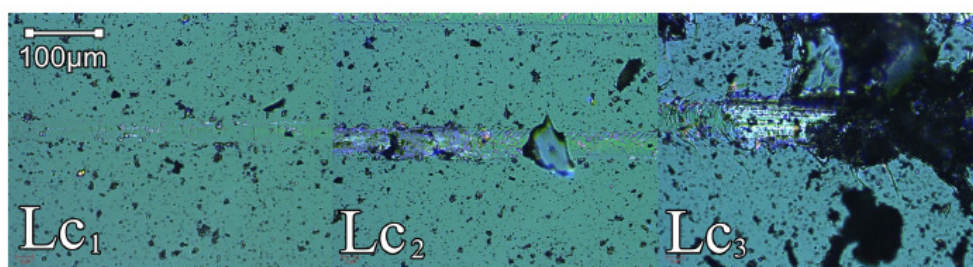


Fig. 3. Optical microscope images of the zones where the adhesion test critical loads were observed – sample SiC\_17.

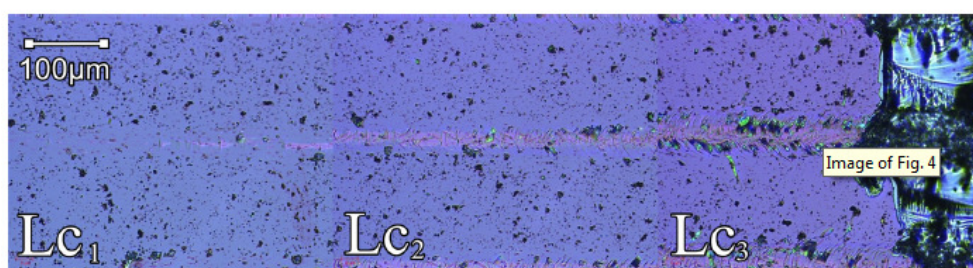


Fig. 4. Optical microscope images of the zones where the adhesion test critical loads were observed – sample SiC\_18.

**Table 3**  
Wear parameters recorded from SiC samples at room temperature and 900°C.

	SiC_17		SiC_18	
T, °C	25	900	25	900
Worn volume (V), mm <sup>3</sup>	0.45	0.32	0.70	0.35
Wear rate, mm <sup>3</sup> /m	9.99E–03	7.14E–03	1.54E–02	7.82E–03
Coefficient of friction (μ)	0.524	0.495	0.668	0.673

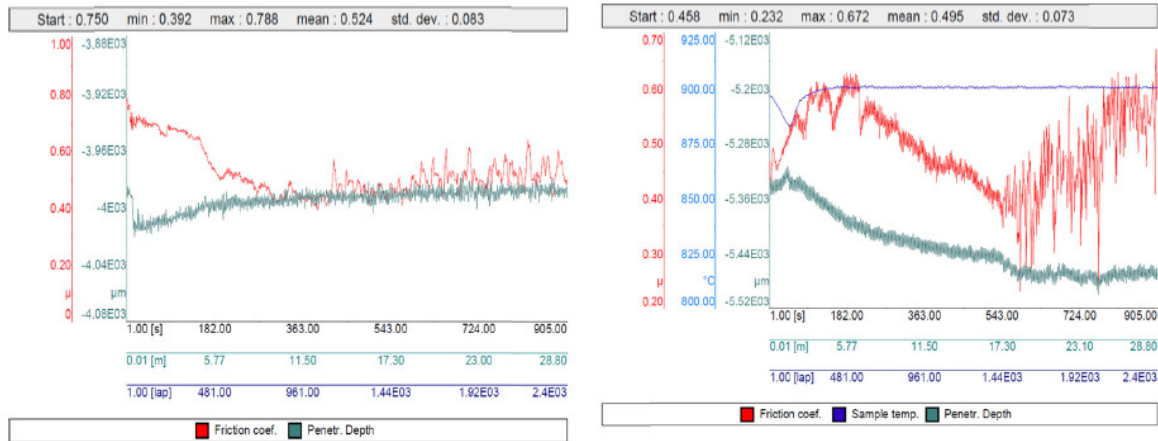


Fig. 5. Friction coefficient, penetration depth and temperature recordings during wear tests performed on SiL17 sample under air ambient at room temperature (left) and 900°C (right).

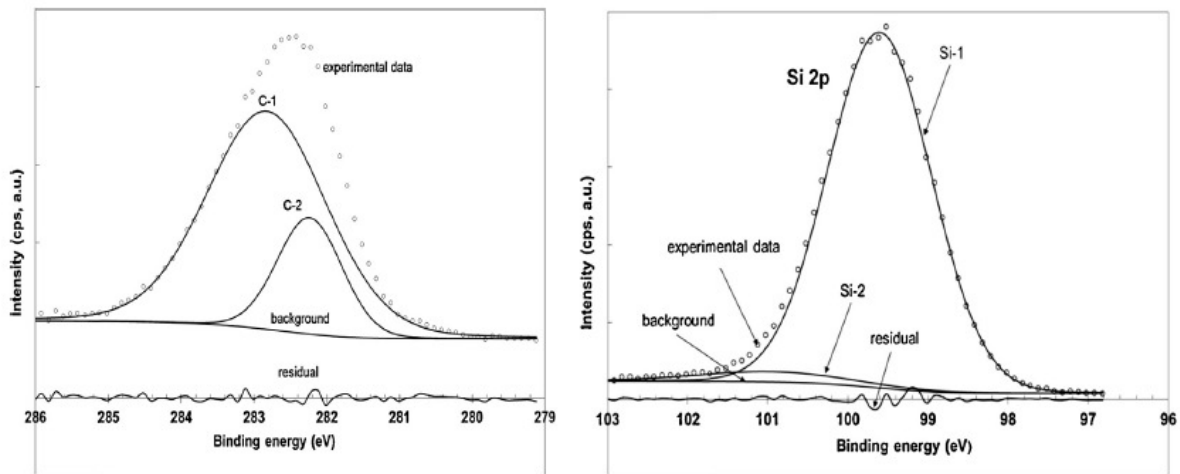


Fig. 6. Simulations of the C 1s and Si 2p high resolution XPS core levels spectra acquired from bulk.

The good wear results could be explained by the results of the analysis of high resolution XPS scans of the C 1s and Si 2p regions acquired from bulk and displayed in Fig. 6. The Si peak was fitted with one high intensity peak located at 99.79 eV, which corresponds to Si-C bonds [1,28,29] and a very small peak, representing around 2% of the large peak area and located at 100.67 eV, most likely indicative of a Si carboxide compound, since the binding energy (BE) is significantly lower than the ~103 eV value corresponding to Si in SiO<sub>2</sub> [1,28,29]. However, at least two peaks of similar areas, corresponding to two chemical bonds for C atoms were necessary to obtain a good fit of the acquired slightly asymmetric C 1s peak. The lower BE of the second smaller area peak was located at 282.31 eV and should correspond to C-Si bonds [1,28,29]. It also showed a significantly smaller FWHM value than the higher BE peak, indicative of better order in this type of compound. The higher BE peak, located at 283.04 eV, which is also wider, must include some contribution from C-C bonds. It is an indication that the deposited SiC films contain a mixture of two regions, one being more ordered and mainly containing Si-C bonds and a more disordered one, also containing a fraction of C-C bonds. Some fraction of this disordered layer may also be a partial result of the long duration Ar ion sputtering of the sample during XPS analysis.

#### 4. Conclusions

The mechanical properties of dense and nanocrystalline SiC films grown at 1000°C by the PLD technique on Si substrates

using a high laser fluence, high repetition rate and high purity atmosphere conditions were investigated. Nanoindentation and scratch test results found that the SiC films were very hard and adherent to the Si substrate, while wear tests showed that films exhibited at 900°C similar friction coefficients and wear rates to those measured at room temperature. The presence of C–C bonds within the bulk, detected by XPS investigations, could account for the good wear behavior. These results show that such SiC films could be successfully used in demanding high temperature applications such as nuclear fuel encapsulation.

### **Acknowledgements**

This work was supported by the IFA-CEA C3-03 grant, UEFIS-CDI Romanian-Hungary bilateral agreement and CNCS – UEFISCDI project Nucleu 2014.

### **References**

- [1] P.R. Poudel, P.P. Poudel, B. Rout, M. El Bouanani, F.D. McDaniel, *Nuclear Instruments and Methods in Physics Research Section B: Beam Interactions with Materials and Atoms* 283 (July) (2012) 93–96.
- [2] C. Ricciardi, G. Fanchini, P. Mandracci, *Diamond and Related Materials* 12 (2003) 1236–1240.
- [3] Y.Y. Wang, K. Kusumoto, C.J. Li, *Physics Procedia* 32 (2012) 95–102.
- [4] J.C. Oh, E. Yun, M.G. Golkovski, S. Lee, *Materials Science and Engineering A* 351(2003) 98–108.
- [5] Q.B. Ma, J. Ziegler, B. Kaiser, D. Fertig, W. Calvet, E. Murugasen, W. Jaegermann, *International Journal of Hydrogen Energy* 39 (2014) 1623–1629.
- [6] M. Ollivier, L. Latu-Romain, M. Martin, S. David, A. Mantoux, E. Bano, V. Souliere, G. Ferro, T. Baron, *Journal of Crystal Growth* 363 (2013) 158–163.
- [7] J. Wang, b. Liu, Y.L. Shao, Z.M. Lu, M.L. Liu, *Nuclear Engineering and Design* 271(2014) 162–165.
- [8] A. Udayakumar, M. Stalin, K. Venkateswarlu, *Surface and Coatings Technology* 219 (2014) 76.
- [9] H. Muto, T. Asano, R.P. Wang, T. Kusumori, *Applied Physics Letters* 87 (2005)(article number: 162106).
- [10] I. Hanyecz, J. Budai, A. Oszkó, E. Szilágyi, Z. Tóth, *Applied Physics A* 100 (2010) 1115–1121.
- [11] Y.S. Katharria, S. Kumar, R.J. Choudhary, R. Prakash, F. Singh, N.P. Lalla, D.M. Phase, D. Kanjilal, *Thin Solid Films* 516 (2008) 6083–6087.



- [12] A.M. Reinecke, M. Lustfeld, W. Lippmann, A. Hurtado, *Nuclear Engineering and Design* 271 (2014) 92–98.
- [13] V. Craciun, E. Lambers, N.D. Bassim, R.H. Baney, R.K. Singh, *Journal of Vacuum Science & Technology A: Vacuum Surface and Films* 19 (2001) 2691–2694.
- [14] G. Monaco, M. Suman, D. Garoli, M.G. Pelizzo, P. Nicolosi, *Journal of Electron Spectroscopy and Related Phenomena* 184 (2011) 240–244.
- [15] G. Socol, A.C. Galca, D. Craciun, M. Hanna, C.R. Taylor, E. Lambers, V. Craciun, *Applied Surface Science* 306 (2014) 66–69.
- [16] W.C. Oliver, G.M. Pharr, *Journal of Materials Research* 47 (1992) 1564–1583.
- [17] P. Du, X.N. Wang, I.K. Lin, X. Zhang, *Sensors and Actuators A: Physical* 176 (2012) 90–98.
- [18] A.V. Singh, S. Chandra, S. Kumar, G. Bose, *Journal of Micromechanics and Micro-engineering* 22 (2012) (article number: 025010).
- [19] Seung Min Han, R. Saha, W.D. Nix, *Acta Materialia* 54 (April (6)) (2006) 1571–1581.
- [20] M. Cabibbo, S. Spigarelli, *Physics Procedia* 40 (2013) 1–8.
- [21] T.L. Oberle, *Journal of Metals* 3 (1951) 438.
- [22] S.J. Bull, *Surface and Coatings Technology* 50 (1991) 25–32.
- [23] G. Dorcioman, G. Socol, D. Craciun, N. Argibay, E. Lambers, M. Hanna, C.R. Taylor, V. Craciun, *Applied Surface Science* 306 (1 July) (2014) 33–36.
- [24] V. Craciun, E. McCumiskey, M. Hanna, C.R. Taylor, *Journal of the European Ceramic Society* 33 (2013) 2223–2226.
- [25] Pavol Kurek, Ján Balko, Ján Dusza, Pavol Sajgalík, Mária Mihaliková, *International Journal of Refractory Metals and Hard Materials* 44 (2014) 12–18.
- [26] Hanqin Liang, Xiumin Yao, Hui Zhang, Xuejian Liu, Zhengren Huang, *International Journal of Refractory Metals and Hard Materials* 44 (2014) 12–18.
- [27] V. Kulikovskiy, V. Vorlicek, R. Ctvrtlik, P. Bohac, J. Suchanek, O. Blahova, L. Jastrabik, *Surface & Coatings Technology* 205 (2011) 3372–3377.
- [28] Y. Matsuda, S.W. King, R.H. Dauskardt, *Thin Solid Films* 531 (2013) 552–558.
- [29] S. Cichon, P. Macháček, B. Barda, M. Kudrnová, *Microelectronic Engineering* 106 (2013) 132–138.